# ECCM21

02-05 July 2024 | **Nantes - France**

## Proceedings of the 21st European Conference on Composite Materials

**Vol 8**

# Special Sessions

**WWW.ECCM21.ORG**

**UNDER THE PATRONAGE OF:**

ESCM European Society For Composite Materials

Association pour les Matériaux Composites AMAC

EuCIA The European Voice of Composites

**WITH THE SUPPORT OF:**

RÉGION PAYS DE LA LOIRE

**ORGANIZED BY:**

CENTRALE NANTES

Nantes Université

**SUPPORTING PARTNER:**

JEC CONNECTING THE WORLD WITH COMPOSITES

## Edited by:

**Prof. Christophe BINETRUY**
ECCM21 Conference Chair
Institute of Civil Engineering and Mechanics (GeM)
Centrale Nantes
Nantes Université

**Prof. Frédéric JACQUEMIN**
ECCM21 Conference Co-Chair
Institute of Civil Engineering and Mechanics (GeM)
Nantes Université

## Published by:

The European Society for Composite Materials (ESCM) and the Ecole Centrale de Nantes.

©2024 ECCM21/The publishers
The Proceedings are published under the CC BY-NC 4.0 license in electronic format only, by the Publisher. The CC BY-NC 4.0 license permits non-commercial reuse, transformation, distribution, and reproduction in any medium, provided the original work is properly cited. For commercial reuse, please contact the authors. For further details please read the full legal code at:
http://creativecommons.org/licenses/by-nc/4.0/legalcode

These Proceedings have an ISBN (owned by the Publisher) and a DOI (owned by the Ecole Centrale de Nantes).

ISBN: 978-2-912985-01-9
DOI: 10.60691/yj56-np80

The Authors retain every other right, including the right to publish or republish the article, in all forms and media, to reuse all or part of the article in future works of their own, such as lectures, press releases, reviews, and books for both commercial and non-commercial purposes.*

## Disclaimer:

The ECCM21 organizing committee and the Editors of these proceedings assume no responsibility or liability for the content, statements and opinions expressed by the authors in their corresponding publication.

# Editorial

Each volume gathers contributions on specific topics:

**Vol 1. Industrial applications**
**Vol 2. Material science**
**Vol 3. Material and Structural Behavior – Simulation & Testing**
**Vol 4. Experimental techniques**
**Vol 5. Manufacturing**
**Vol 6. Multifunctional and smart composites**
**Vol 7. Life cycle performance**
**Vol 8. Special Sessions**

**Prof. Christophe BINETRUY**
ECCM21 Conference Chair
*Institute of Civil Engineering and Mechanics (GeM)*
*Centrale Nantes*
*Nantes Université*

**Prof. Frédéric JACQUEMIN**
*ECCM21 Conference Co-Chair*
*Institute of Civil Engineering and Mechanics (GeM)*
*Nantes Université*

This collection contains the proceedings of the 21st European Conference on Composite Materials (ECCM21), held in Nantes, France, July 2-5, 2024. ECCM21 is the 21st in a series of conferences organized every two years by the members of the European Society of Composite Materials (ESCM). As some of the papers in this collection show, this conference reaches far beyond the borders of Europe.

The ECCM21 conference was organized by the Nantes Université and the Ecole Centrale de Nantes, with the support of the Research Institute in Civil and Mechanical Engineering (GeM).

Nantes, the birthplace of the novelist Jules Verne, is at the heart of this edition, as are the imagination and vision that accompany the development of composite materials. They are embodied in the work of numerous participants from the academic world, but also of the many industrialists who are making a major contribution to the development of composite materials. Industry is well represented, reflecting the strong presence of composites in many application areas.

With a total of 1,064 oral and poster presentations and over 1,300 participants, the 4-day event enabled fruitful exchanges on all aspects of composites. The topics that traditionally attracted the most contributions were fracture and damage, multiscale modeling, durability, aging, process modeling and simulation and additive manufacturing.

However, the issues of energy and environmental transition, and more generally the sustainability of composite solutions, logically appear in this issue as important contextual elements guiding the work being carried out. This includes bio-sourced composites, material recycling and reuse of parts, the environmental impact of solutions, etc.

We appreciated the high level of research presented at the conference and the quality of the submissions, some of which are included in this collection. We hope that all those interested in the progress of European composites research in 2024 will find in this publication sources of inspiration and answers to their questions.

# Under the Patronage of:

ESCM
European Society For Composite Materials

Association pour les Matériaux Composites

EuCIA
The European Voice of Composites

Organized by:

CENTRALE NANTES

Nantes Université

With the support of:

RÉGION PAYS DE LA LOIRE

Supported by:

EMC2

JEC
CONNECTING THE WORLD WITH COMPOSITES

# Sponsored by:

Bronze Partner:

BRUKER

INSTRON

MatchID
Metrology beyond colors

Other partners:

CAPACITÉS
De la recherche à l'innovation

CARBON AXIS

CETIM

Depestele

EikoSim

ELSEVIER

FAIRMAT

metravib
material testing

NOVITOM

Quantiflex
simulations

Surface Measurement Systems
World Leader in Sorption Science

# Hosting Organizations

## Conference chairs

**Prof. Christophe BINETRUY**
ECCM21 Conference Chair
Institute of Civil Engineering and Mechanics (GeM)
Centrale Nantes
Nantes Université

**Prof. Frédéric JACQUEMIN**
ECCM21 Conference Co-Chair
Institute of Civil Engineering and Mechanics (GeM)
Nantes Université

## International Scientific Committee

Malin Akermo (Sweden)
Remko Akkerman (Netherlands)
Andrey Aniskevich (Latvia)
Leif Asp (Sweden)
Emmanuel Baranger (France)
Janice Barton (UK)
Johnny Beaugrand (France)
Andrea Bernasconi (Italy)
Christophe Binetruy (France)
Thomas Bohlke (Germany)
Alain Bourmaud (France)
Nicolas Boyard (France)
Joël Breard (France)
Richard Butler (UK)
Baris Caglar (Netherlands)
Pedro Camanho (Portugal)
Pierpaolo Carlone (Italy)
Paolo Andrea Carraro (Italy)
Valter Carvelli (Italy)
Nuno Correia (Portugal)
Gergely Czél (Hungary)
Clemens Dransfeld (Netherlands)
Sylvain Drapier (France)
Klaus DRECHSLER (Germany)
Andreas ECHTERMEYER (Norway)
Paolo Ermanni (Switzerland)
Martin Fagerström (Sweden)
Ewald Fauster (Austria)
Julien Ferec (France)
Antonio Ferreira (Portugal)
Bodo Fiedler (Germany)
Stefanos Giannis (UK)
Nathalie Godin (France)
Carlos Gonzalez (Spain)
Sotirios Grammatikos (Norway)
Christoph Greb (Germany)
Emile Greenhalgh (UK)
Gianmarco Griffini (Italy)
Stephen Hallett (UK)
Nahiene Hamila (France)
Roland Hinterhoelzl (Austria)
Martin Hirsekorn (France)
Darko Ivančević (Hungary)
Frédéric Jacquemin (France)
Mikko Kanerva (Finland)
Luise Karger (Germany)
Vassilis Kostopoulos (Greece)
Theodosia Kourkoutsaki (Germany)
Thomas Kruse (Germany)
Ugo Lafont (France)
Jacques Lamon (France)
Frédéric Laurin (France)
Antoine Le Duigou (France)
Stepan Lomov (Belgium)
Theodoros Loutas (Greece)
Staffan Lundstrom (Sweden)
António Marques (Portugal)
David May (Germany)
Véronique Michaud (Switzerland)
Jörg Mussig (Germany)
Thomas Neumeyer (Germany)
Philippe Olivier (France)
Alkiviadis Paipetis (Greece)
Federico Paris (Spain)
Chung Hae Park (France)
John-Alan Pascoe (Netherlands)
Alessandro Pegoretti (Italy)
Ton Peijs (UK)
Rob Pierce (Denmark)
Soraia Pimenta (UK)
Silvestre Pinho (UK)
Gerald Pinter (Austria)
Connie Qian (UK)
Marino Quaresimin (Italy)
Andrew Rhead (UK)
Paul Robinson (UK)
Essi Sarlin (Finland)
Yentl Swolfs (Belgium)
Sofia Teixeira du Freitas (Netherlands)
Julie Teuwen (Netherlands)
Ole Thomsen (UK)
Stavros Tsantzalis (Greece)
Konstantinos Tserpes (Greece)
Albert Turon (Spain)
Julien van Campen (Netherlands)
Wim Van Paepegem (Belgium)
Anastasios Vassilopoulos (Switzerland)
Ignaas Verpoest (Belgium)
Michael Wisnom (UK)
Dimitrios Zarouchas (Netherlands)
Daiva Zeleniakiene (Lithuania)
Dan Zenkert (Sweden)

## Local Organizing Committee

Suresh Advani
Romain Agogué
Sylvain Chataigner
Sébastien Comas-Cardona
Sofiane Guessasma
Suzanne Laïk
Philippe Le Bot
Mael Peron
Luisa Silva
Vincent Sobodka
Alexandre Ripoche
Elena Syerko

# Table of Contents

# PROBING COMPRESSIVE BEHAVIOUR AND FAILURE IN SINGLE FIBRE CARBON FIBER COMPOSITES: IN-DEPTH ANALYSIS USING *IN SITU* LASER RAMAN SPECTROSCOPY

Cameron G. Woodgate[1], Richard S. Trask[1], Milo S.P. Shaffer[2], Stephen J. Eichhorn[1]

[1]Bristol Composites Institute, School of Civil, Aerospace and Design Engineering, University of Bristol, University Walk, Bristol BS9 1TR, UK.
Email: cameron.woodgate@bristol.ac.uk, r.s.trask@bristol.ac.uk, s.j.eichhorn@bristol.ac.uk
[2]Department of Materials and Department of Chemistry, Imperial College London, South Kensington Campus, London, SW7 2AZ, UK
Email: m.shaffer@imperial.ac.uk

**Keywords:** Carbon Fibre, compression, interface, Raman spectroscopy, micromechanics

**Abstract**
Compressive failure of fibres in unidirectional composites is often characterised by microbuckling and the formation of kink bands. Developing insight into the behaviour of reinforcing fibre and the fibre-matrix interface before, during, and after failure is crucial for enhancing compressive performance. Direct mechanical testing of single fibres is limited due to scale considerations, necessitating alternative approaches, additionally, characterising interfacial behaviour in compressive loading lacks a direct quantitative method.

In this study, Raman spectroscopy is utilised as a non-contact method for characterising micromechanical behaviour and interfacial responses during compressive loading. *In situ* laser Raman spectroscopy is employed to investigate compressive stress-strain behaviour of single fibres as well as generate spatially resolved stress maps of single carbon fibres under compression. Two experimental setups are discussed: a four-point bending setup for static Raman analysis and a uniaxial compression setup for stress map generation. High-resolution Raman stress maps, scanning electron microscopy, and confocal laser scanning microscopy are used to examine the evolution of failure of high modulus carbon fibres. This research contributes to a deeper understanding of compressive performance in carbon fibre composites, crucial for advancing their design and future applications.

## 1. Introduction

The compressive performance of unidirectional carbon fibre reinforced polymer composites (CFRPs) is often suboptimal when compared to the same material's tensile performance. CFRPs often exhibit compressive strengths that are ~60% of their tensile strength [1]. To enhance compressive properties of CFRPs it is critical to understand the behaviour of reinforcing fibres and their interface with a matrix, prior to, during and post-failure. However, direct mechanical testing of fibres is challenging in compression due to their scale and aspect ratio [2]. There are also few direct measurement techniques to assess interfacial micromechanics in compressive loading conditions. *In-situ* laser Raman spectroscopy is one such technique and can be applied as an indirect non-contact stress sensing approach. Raman scattering is especially effective for graphitic materials such as carbon fibres [3], providing e information about the underlying atomic structure and bonding. When subjecting a single carbon fibre to mechanical loading, local fibre stress can be determined by measuring the shift in frequency of a particular Raman band, the graphitic or 'G' band, located at ~1580 $cm^{-1}$. This shift in frequency corresponds to compression of in-plane atomic bonds in the graphitic lattice of the carbon structure, leading to phonon hardening, increasing the frequencies of scattered light and a resulting shift of the G band's spectral position to a higher Raman wavenumber position [4]. By calibrating this shift against strain, stress can be derived using elastic deformation principles. By collecting spectra at spatial increments, point-to-point stress maps can then be produced along a length of fibre subjected to

mechanical loading within a model composite. This study employs *in-situ* Raman spectroscopic spatially resolved stress maps of single carbon fibres subjected to compressive loading to investigate fibre micromechanics and interfacial behaviours.

## 2. Materials and Methods

### 2.1 Materials

Two commercial PAN-based high modulus carbon fibres were used in this study; namely M46J and M55J fibres (Toray Advanced Composites, NL). Two sample types are prepared, a poly(methyl methacrylate) (PMMA) beam for four-point bending experiments and an epoxy prism for uniaxial compression analysis. PMMA was supplied by Merck (DE) and the epoxy resin formulation used was Araldite® LY5052 resin and Aradur® 5052CH hardener supplied by Huntsman Corporation (US). The resin contained 50-70 % phenol polymer with formaldehyde, glycidyl ether and 30-50% 1,4-Bis(2,3-epoxypropoxy)butane, and a hardener. The hardener comprised 50-70% 2,2'dimethyl- 4,4'-methylenebis(cyclohexylamine), 30-50% 3-aminomethyl-3,5,5-trimethylcyclohexylamine, 3-5%, 2,4,6-tris(dimethylaminomethyl)phenol and 1-3% salicylic acid. A non-silicone mould release agent, Ambersil Formula 10, (RS Components Ltd, Bristol GB) was used and C4A-06-015SLA-120-39P strain gauges, supplied by Micro-Measurements group UK Ltd (Basingstoke, GB) were utilised to measure strain during deformation of the model composites.

### 2.2 Methodology

*2.2.1 Sample preparation*

Two sample types were prepared for Raman analysis; PMMA four-point bending beams and epoxy prisms for direct compression, both with a single fibre embedded near the surface. Beams were laser cut from a PMMA sheet into dimensions of 64 × 12.5 × 3.1 mm, following standardised dimensions ASTM D6272-17 [5]. Single fibres were manipulated onto the surface of the beam and aligned parallel to its long edge and secured in place with adhesive tape. To encapsulate the fibre onto the beam's surface a 5 % by weight PMMA-acetone solution was prepared and placed over the fibre via pipette and left at room temperature to evaporate away the acetone, leaving a thin encapsulating layer of PMMA over the fibre. A strain gauge was adhered via a cyanoacrylate adhesive to the same face of the beam, with the gauge's longest length parallel to the fibre axis. The resulting beam and bending experiment is shown in Figure 1a.

Single fibre epoxy prisms were prepared by first casting the base epoxy prism in a silicone mould, coated in release agent. The two epoxy components, resin LY5052 and hardener 5052CH, were thoroughly mixed in a ratio of 100:38 parts by weight, following the manufacturer's guidelines. The mixture was degassed in a vacuum chamber at 700 mm.Hg, for 30 minutes, poured into the coated silicone mould and left at room temperature and pressure for 7 days to cold cure. The resulting prisms had dimensions of 12 × 6 × 6 mm, following ASTM D695-15 [6]. To embed a single fibre in the epoxy resin, a short filament (3-5 mm) was manipulated onto the surface of a cured prism, aligned parallel and centrally with the long edge of the prism and secured in place with adhesive tape. A thinned epoxy solution was prepared by first following the same mixing and degassing procedure as discussed above, then mixing the degassed epoxy with acetone in a ratio of 25:75 parts by weight epoxy to acetone. Thinned epoxy was dropped over the fibre using an adjustable air-displacement pipette in a volume of 30 µL, removing the adhesive tape prior to dropping the acetone, ensuring the fibre remained on the prism. Epoxy-acetone solution was spread across the prisms' surface, ensuring the solution was evenly spread to a uniform thickness. The fibre was gently manipulated to ensure the fibre was aligned with the prisms long edge. Encapsulated fibre samples were left for 7 days at room temperature to allow the epoxy to cold cure, minimising residual stresses.

Following the cold cure, a post-cure step of 60°C for 6 hours was completed enabling a consistent cure across all samples. A strain gauge was then adhered to the prism, parallel to the fibre length, as shown in Figure 1b.

*2.2.2 In-situ Raman analysis*

Raman spectroscopy was carried out using a Renishaw inVia micro-Raman spectrometer, with a 532 nm, 2.33 eV DPSS diode laser with a maximum power of 0.5 W. Software used to control the spectrometer and motorised stage was the WiRe 4.1 HF7241 2014 interface. The CCD used had a grating with 1800 lines/mm and a long working distance 50× lens with a numerical aperture of 0.5 was utilised for the measurements, resulting in an average spot size of 0.8 µm. Prior to measurements being carried out, the system was calibrated against a silicon (Si) wafer using a spectral band located at 520 $cm^{-1}$. Any drift in the position of this band was accounted for by offsetting the CCD's grating position to shift to the reference value.

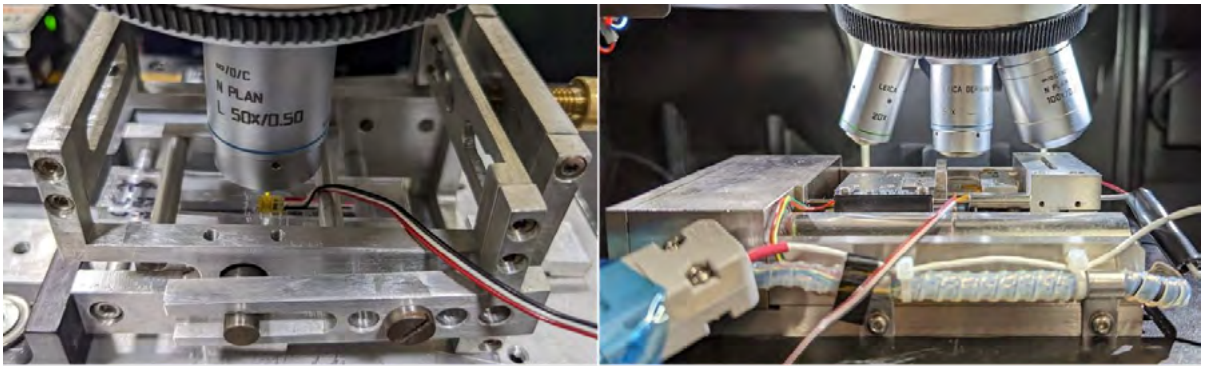


(a) (b)

**Figure 1.** Two experimental setups utilised for *in situ* Raman spectroscopy. a) A four-point bending rig with a PMMA beam with a single fibre encapsulated on the compressive face of the beam and b) a uniaxial compression setup, utilising a Deben 5 kN microtester and epoxy prisms with an embedded single fibre.

Four-point bending PMMA beams with single fibres embedded were utilised to calibrate the G-band strain sensitivity for the fibres investigated. An in-house fabricated, manually operated four-point bending rig was used (Figure 1a), where bending was applied in resulting strain steps of -0.034%, measured via a strain gauge adhered to the compressive face of the beam. *In situ* Raman measurements were taken in a single position in the centre of the fibre's length, with measurement conditions ranging from 2-10 seconds with a laser power of 1-10%. Once spectra have been collected, spectral band information was derived via deconvolution of the spectrum into peaks corresponding to vibrational modes, listed in Table 1. Pseudo-Voigt functions were used to fit these bands, as described elsewhere [7].

Point-to-point stress mapping was carried out utilising an epoxy prism sample geometry, which were subjected to uniaxial compression via use of a Deben MICROTEST tensile compression stage, fitted with a 5 kN loadcell, pictured in Figure 1b. This setup was installed on the motorised stage of the Raman microscope. Full lengths of embedded short fibres were mapped at increasing levels of compressive deformation to evaluate how local fibre compressive stress evolved. Samples were first mapped with no applied loading, where spectra were collected every 5 µm over a range 0-200 µm, starting at the end of the fibre, then every 50 µm until 200 µm from the end of the opposite end of the fibre.

**Table 1.** Vibrational bands present within the Raman spectra region of interest. Corresponding vibrational modes for each band are described with peak position fitting bounds denoted. Peak full widths at half maximum are constrained between 10 to 1000 $cm^{-1}$, peaks are positive and a linear background of y = 0 was used.

| Vibrational band | Peak position [Bounds] ($cm^{-1}$) | Vibrational mode |
|---|---|---|
| G | ~1580 [1500-1650] | Ideal graphitic lattice ($E_{2g}$ symmetry) |
| D | ~1350 [1300-1400] | Disordered graphitic lattice ($A_{1}g$ symmetry), associate with graphene layer edges |
| D′ | ~1620 [1590-1630] | Disordered graphitic lattice (surface graphene layers, $E_{2g}$ symmetry) |
| D″ | ~1500 [1400-1550] | Amorphous carbon |
| I | ~1200 [1050-1300] | Disordered graphitic lattice ($A_{1g}$ symmetry) |

Measurement conditions ranged from 2-10 second scans with a 1-10% laser power, depending on the sample's fibre depth in epoxy). This map was collected both as a baseline and to measure possible residual stresses within the fibre from the curing of the epoxy resin. Load was then applied by increasing the cross-head displacement (in compression) to control the prism's compressive strain, measured via a Micro-Measurements D4 Data Acquisition Conditioner. Spectra were taken during loading at specific strain increments, in strain steps of -0.034 %. Maps and Raman band positions were taken in strain increments of -0.25 %. Maps of loaded fibres had inter-spectra spacings of 2, 5 and 50 μm from 0-100, 105-400, and 450 μm, to the centre of the fibre, respectively. The same resolutions were repeated for the other half of the fibre, resulting in the entire length of fibre being mapped, with higher mapping resolution at the ends of the fibres. Each individual spectrum within each map had the position of the G band discerned using the method described above and in Table 1 and the position of the G band with respect to position along the fibre is collected.

*2.2.4 Confocal Laser Scanning Microscopy*

Confocal Laser scanning microscopy (CLSM) was utilised here to investigate both fibre depth in epoxy prism samples to check for sample consistency and investigate post-failure fibre geometries. CLSM was carried out using a Leica SP8 AOBS confocal laser scanning microscope. Fibre depths in epoxy were measured using a 10× air gap lens and a 50× long working distance lens, using an Argon ion 488 nm laser. Images were analysed using ImageJ.

## 3. Results and Discussion

### 3.1 *In situ* Raman investigations

*3.1.1 Four-point bending*

The four-point bending experimental setup was used to obtain both a G band strain sensitivity calibration and additionally to derive compressive stress within single fibres undergoing compressive loading. Compressive stress-strain curves for the two fibres investigated here have been reported elsewhere [8]. By comparing the deconvoluted position of the carbon fibre's G band to the level of compressive strain, obtained from the strain gauge adhered to the surface of the PMMA beam, a G-band strain calibration was obtained (in $cm^{-1}$/%). This method assumes that the strain experienced by the fibre is the same as the strain gauge reading. G band strain sensitivities are reported in Table 2, obtained via fitting linear regressions to G band Raman wavenumber shift versus compressive strain data. Due to non-linear response of carbon fibres in compressive loading, the curves were split into two regimes to account for compressive modulus 'softening' [9].

To utilise the G band strain sensitivities ($\frac{\Delta G}{\Delta \varepsilon_f}$) to derive stress, $\sigma_f$, a previously reported approach was used [9].

$$\Delta\sigma_f = \Delta G \times \frac{\Delta\varepsilon_f}{\Delta G} \times \frac{\Delta\sigma_f}{\Delta\varepsilon_f} \quad (1)$$

where $\Delta G$ is the shift in the position of the G band and $\frac{\Delta\sigma_f}{\Delta\varepsilon_f}$ is the tensile Young's modulus of the measured fibre.

**Table 2.** G band strain sensitivities for two fibres under investigation.

| Fibre | Non-linear onset strain (%) | Initial G Band Sensitivity ($cm^{-1}$/%) | High Strain G Band Strain Sensitivity ($cm^{-1}$/%) |
|---|---|---|---|
| M46J | 0.47 | 9.64 ± 0.3 | 4.27 ± 0.4 |
| M55J | 0.41 | 11.68 ± 0.7 | 6.00 ± 1.9 |

*3.1.1 Point-to-point Raman stress mapping*

Once the G band strain sensitivities reported in Table 2 were obtained, point-to-point stress mapping was carried out. G band positions were collected along a short length of a single fibre compared to a zero stress position, obtaining $\Delta G$. Equation 1 was then used to derive local compressive stress. These data were then compiled into a map such as that seen in Figure 2a.

A shear-lag model was used to fit a trend to the data [10], from which, interfacial shear stress (IFSS) was determined using a force balance approach (Figure 2b). From these derived IFSS curves, quantifiable interfacial parameters such as the maximum shear stress ($\tau_{max}$) and transfer length ($L_t$) were obtained, for which there are very few alternative techniques to measure in compressive loading.

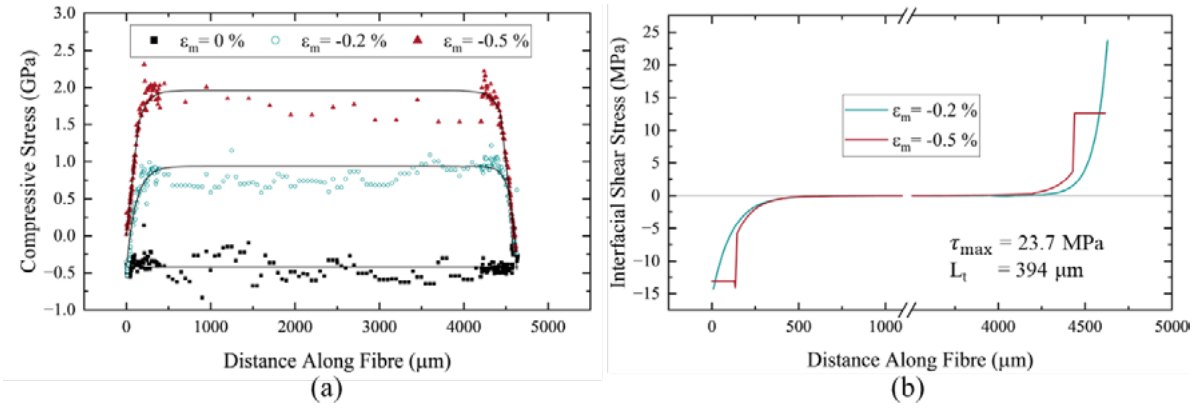


**Figure 2.** Point-to-point Raman stress maps of a single M46J fibre undergoing uniaxial compressive loading, where (a) demonstrates how local stresses evolve over increasing levels of applied loading and (b) the derived IFSS information for the mapped fibre. Solid lines in (a) are fitting a micromechanical model reported elsewhere [10].

Additionally, using this approach, physical changes to the interface can be identified through stress mapping, such as in Figure 2a where a linearisation of the stress uptake at $\varepsilon_m$= -0.5 % occurs at the ends of the fibre. This linearisation corresponds to a debonded or partially debonded interface, where the stress transfer between the matrix and interface becomes frictional rather than shear-based. The corresponding constant interfacial shear stress in Figure 2b indicates the shear stress at which the IFSS is a maximum, overcoming the interfacial shear strength, causing matrix-interface debonding to occur.

Point-to-point mapping is a versatile technique for single fibre model composites in compression as the maximum spatial resolution is in the range of 0.5-1 μm, depending on the Raman spectrometer's laser spot size. By utilising the equipment at its maximum resolution, micromechanical failure modes, such as compressive fragmentation, can be investigated as failure evolves. An example high resolution stress map for an M46J fibre undergoing compressive fragmentation is shown in Figure 3.

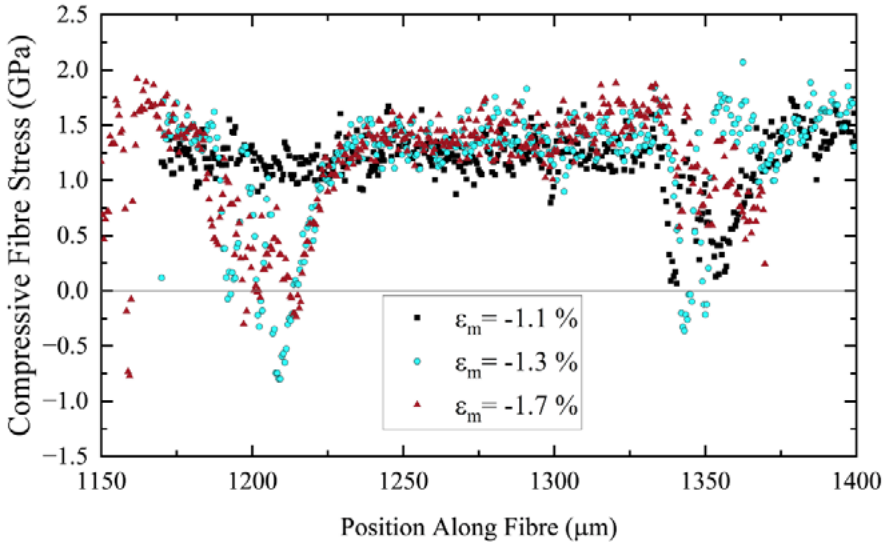


**Figure 3.** Highly spatially resolved Raman stress map of an M46J HM fibre undergoing compressive failure. The map shows how the local stress state evolves over increasing compressive loads, with a measurement every 0.5 μm.

Features that develop during compressive failure of HM fibres can be tracked and investigated using high-resolution mapping, such as the development of a break (seen developing in Figure 3 between 1150-1250 μm), individual fragment shear-lag profiles (1200-1350 μm) and inter-fragment features (1350-1370 μm). Combining high resolution Raman stress maps of HM fibre fragmentation with imaging techniques such as CLSM (Figure 4), provides further insight into how fibres fail in compression, allowing investigation of geometric configurations of post-failed fibres.

CLSM allows 3D analysis of the features of HM fibre fragmentation which, in turn, will allow a more thorough understanding to the failure progression experienced by single fibres, by combining the images with high resolution Raman maps of fragment evolution, which only gives a 2D view of fragmentation behaviour (Raman mapping is only carried out in 1 dimension along a fibre's length).

A combination of analytical techniques, such as those used here, will allow a more in-depth understanding of how single fibre model composites, such as those used here, and multi-fibre, macro composite failure initiates, propagates and how ultimate failure occurs.

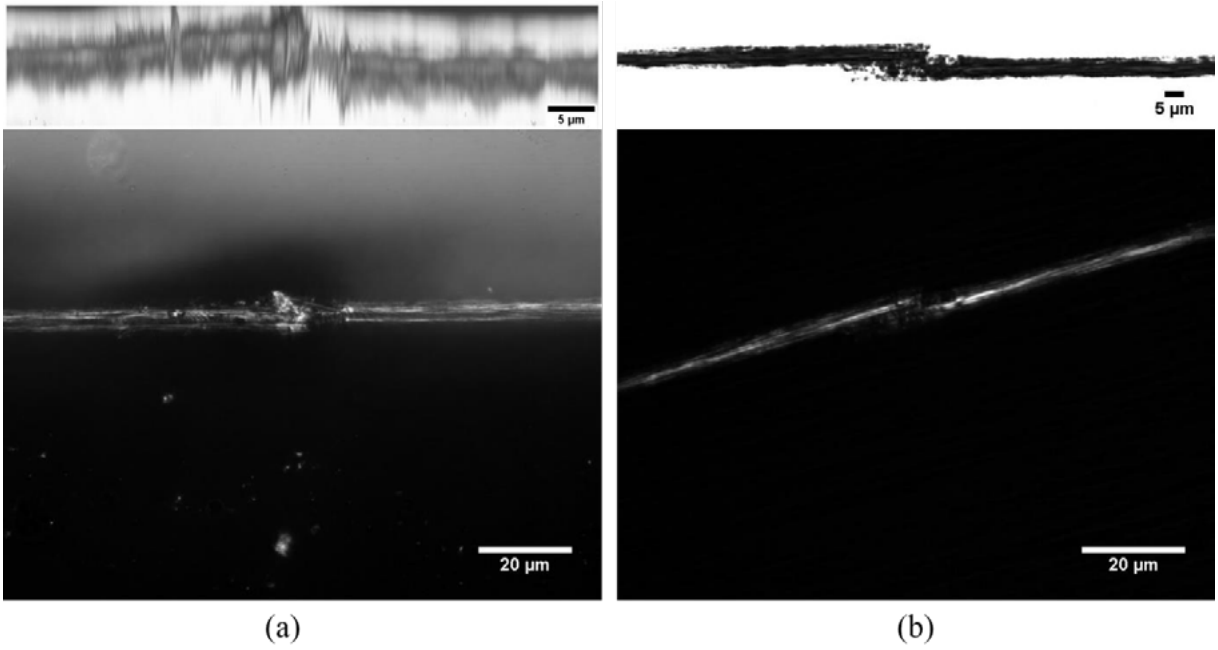


**Figure 4.** Confocal laser scanning microscopy images of example HM fibre fragmentation features, (a) a break location in a fragmented M46J fibre and (b) a fragment-slip feature, imaged in a fragmented M55J fibre sample. Top images are the XY projections of the features imaged in the bottom image, which is an averaged z-projection of the stack.

## 4. Conclusions

The utilisation of *in situ* Raman spectroscopic mapping method to characterise both fibre micromechanical behaviour and interfacial properties is a versatile technique capable of highly spatially resolved stress mapping. This approach allows for tracking the initiation and propagation of fibre compressive fragmentation. When combined with confocal laser scanning microscopy, it enables a more comprehensive analysis of fragmentation behaviour by imaging post-failure geometric fibre configurations. This integrated methodology provides valuable insights into the mechanical response of carbon fibre-reinforced polymer composites under compression, facilitating advancements in composite design and performance optimisation.

## Acknowledgments

The authors kindly acknowledge the funding for this research provided by UK Engineering and Physical Sciences Research Council (EPSRC) programme Grant EP/T011653/1, Next Generation Fibre-Reinforced Composites: a Full Scale Redesign for Compression (NextCOMP) a collaboration between Imperial College London and University of Bristol. For the purpose of open access, the author has applied a Creative Commons Attribution (CC BY-NC 4.0) license to any author accepted manuscript version arising. The authors also acknowledge the support of Henry Royce Institute at Imperial College London for the use of confocal microscope.

## References

[1] N.A. Fleck, Compressive Failure of Fiber Composites. *Adv. Appl. Mech.* volume 33: 43–117, 1997.

[2] S. Nunna, A.R. Ravindran, J. Mroszczok, C. Creighton, R.J. Varley, A review of the structural factors which control compression in carbon fibres and their composites, *Compos. Struct.* volume 303, 116293, 2023.

[3] Z. Li, L. Deng, I.A. Kinloch, R.J. Young, Raman spectroscopy of carbon materials and their

composites: Graphene, nanotubes and fibres, *Prog. Mater. Sci.* volume 135, 101089, 2023.

[4] T.M.G. Mohiuddin, A. Lombardo, R.R. Nair, A. Bonetti, G. Savini, R. Jalil, N. Bonini, D.M. Basko, C. Galiotis, N. Marzari, K.S. Novoselov, A.K. Geim, A.C. Ferrari, Uniaxial strain in graphene by Raman spectroscopy: G peak splitting, Grüneisen parameters, and sample orientation, *Phys. Rev. B - Condens. Matter Mater. Phys.,* volume 79, 1–8, 2009.

[5] ASTM D6272, Standard Test Method for Flexural Properties of Unreinforced and Reinforced Plastics and Electrical Insulating Materials by Four-Point Bending, *Man. Hydrocarb. Anal. 6th Ed. 02*, 545-545–3, 2008.

[6] ASTM D695-15 Standard test method for compressive properties of rigid plastics, *ASTM Int. 08,* 1–7, 2015.

[7] Z.E. Brubaker, J.J. Langford, R.J. Kapsimalis, J.L. Niedziela, Quantitative analysis of Raman spectral parameters for carbon fibers: practical considerations and connection to mechanical properties, *J. Mater. Sci.,* volume 56, 15087–15121, 2021.

[8] C.G. Woodgate, R.S. Trask, M.S.P. Shaffer, S.J. Eichhorn, Compressive Characterisation of Single Carbon Fibres and Their Composite Interfaces Via in Situ Raman Spectroscopy, *ICCM Int. Conf. Compos. Mater*. 2023.

[9] F. Tanaka, T. Okabe, H. Okuda, M. Ise, I.A. Kinloch, T. Mori, R.J. Young, The effect of nanostructure upon the deformation micromechanics of carbon fibres, *Carbon N. Y.,* volume 52, 372–378, 2013.

[10] M.R. Piggott, Reinforcement Processes, in: Load-Bearing Fibre Compos., *Elsevier*: pp. 83–99, 1980.

# ECCM21

02-05 July 2024 | **Nantes - France**

Volume 8

# Special Sessions

ISBN: 978-2-912985-01-9
DOI: 10.60691/yj56-np80